Available online at website: https://journal.bcrec.id/index.php/bcrec

Bulletin of Chemical Reaction Engineering & Catalysis, 21 (3) 2026, 507-515

Original Research Article

Optimized Cobalt-Loaded Palm Oil Fuel Ash (Co/POFA) Catalyst for Syngas Production via Ethanol Dry Reforming

Mohamad Irfan Nordin[1], Asmida Ideris[1], Muhammad Shahim Azim Razat[1], Siti Jamilatun[2], Joko Pitoyo[2], Utaminingsih Linarti[3], Nurul Ainirazali[1,4*]

[1]Faculty of Chemical and Process Engineering Technology, Universiti Malaysia Pahang Al-Sultan Abdullah, 26300 Gambang, Pahang, Malaysia.
[2]Department of Chemical Engineering, Faculty of Industrial Technology, Universitas Ahmad Dahlan, Jl. Jend. Ahmad Yani, Banguntapan, Bantul, Yogyakarta, Indonesia 55166.
[3]Department of Industrial Engineering, Faculty of Industrial Technology, Universitas Ahmad Dahlan, Jl. Jend. Ahmad Yani, Banguntapan, Bantul, Yogyakarta, Indonesia 55166.
[4]Centre of Excellence for Advanced Research in Fluid Flow (CARIFF), Universiti Malaysia Pahang Al-Sultan Abdullah, 26300 Gambang, Pahang, Malaysia.

Received: 3rd February 2026; Revised: 12th March 2026; Accepted: 12th March 2026
Available online: 15th March 2026; Published regularly: October 2026

Abstract

Converting biogenic carbon and captured CO_2 into synthesis gas (syngas) via ethanol dry reforming (EDR) offers a pathway to low-carbon fuels, but catalyst instability and coking remain key barriers. Palm-oil fuel ash (POFA), a silica-rich agro-industrial waste, was investigated in this study as a support material for cobalt loading and to evaluate its performance in EDR. Co/POFA catalysts containing 5-20 wt % Co was prepared by ultrasonic-assisted incipient wetness, calcined, and tested for EDR at 750 °C. Nitrogen physisorption, FT-IR, and post-reaction TGA were employed to correlate catalyst texture, surface chemistry, and thermal stability with ethanol and CO_2 conversion, as well as H_2 and CO yields. Maximal, durable activity occurred at the intermediate Co loading (15 wt%), where ethanol and CO_2 conversions were ~72% and 80% initially and remained ~50% and 68% after 5 h, the ~48% H_2 yield was sustained, consistent with a loading that maximizes accessible Co sites without incurring mesopore transport limitations. Lower loading of 5 wt % Co was site-limited and heavily coked, whereas excessive loading of 20 wt % Co showed rapid deactivation attributed to pore blockage and cobalt agglomeration despite minimal coke. Optimizing cobalt dispersion on conditioned POFA enables stable syngas production under demanding EDR conditions, validating Co/POFA as a viable waste-derived catalyst for circular, CO_2-utilizing hydrogen generation.

Keywords: EDR; Cobalt catalyst; Oil Palm ash (OPA); Waste-derived support; CO_2 valorization; Hydrogen production

How to Cite: Nordin, M. I., Ideris, A., Azim Razat, M. S., Jamilatun, S., Pitoyo, J., Linarti, U., Ainirazali, N. (2026). Optimized Cobalt-Loaded Palm Oil Fuel Ash (Co/POFA) Catalyst for Syngas Production via Ethanol Dry Reforming. *Bulletin of Chemical Reaction Engineering & Catalysis*, 21 (3), 507-515. (DOI: 10.9767/bcrec.20662)

Permalink/DOI: https://doi.org/10.9767/bcrec.20662

1. Introduction

Deep decarbonization of the energy system will require carbon-neutral molecular fuels and scalable vectors for long-distance energy transport. Hydrogen is a leading candidate, yet most global H_2 supply is still derived from fossil feedstocks with significant CO_2 emissions [1]. Accordingly, intensified research has focused on renewable hydrogen routes that integrate waste carbon streams, improve lifecycle performance, and leverage existing liquid-fuel logistics [2]. Bioethanol produced at commercial scale from sugar, starch, and increasingly lignocellulosic resources offers an attractive platform molecule for such strategies [3]. When co-processed with CO_2, it can be upgraded thermochemically to synthesis gas (syngas), a versatile intermediate for Fischer-Tropsch, methanol, higher alcohols, and emerging e-fuels pathways [4].

Ethanol dry reforming (EDR) couples bioethanol with CO_2 according to the overall stoichiometry: $C_2H_5OH + CO_2 \rightarrow 3CO + 3H_2$ ($\Delta H°$

* Corresponding Author.
Email: ainirazali@umpsa.edu.my (N. Ainirazali)

> 0), delivering a syngas stream with an intrinsic H_2/CO ratio near unity that advantageous for downstream carbonylation chemistry and tunable through secondary reactions [5]. The process is strongly endothermic, requiring elevated temperatures (>700 °C) to overcome kinetic barriers and suppress thermodynamic limitations [6]. Under these conditions, however, undesired pathways compete between ethanol dehydration to ethylene, cracking to CH_4 and light hydrocarbons, Boudouard carbon formation ($2CO \rightarrow C + CO_2$), and methanation/shift equilibria that erode syngas yield [7]. Consequently, catalyst selection is critical for high activity for C-C and O-H bond activation must be paired with resistance to sintering, carbon deposition, and chemical poisoning to achieve stable operation [8].

Noble metals (Rh, Ru, Pt) exhibit excellent reforming performance but remain cost-prohibitive for bulk deployment [9]. Nickel (Ni) has been widely studied yet is notoriously prone to filamentous coke growth under CO_2-rich feeds [10]. Cobalt (Co) occupies an intermediate position: more affordable than noble metals and often more resistant to carbon formation than Ni under oxidative reforming environments, while displaying strong activity for C-C scission and dehydrogenation in alcohol reforming [12]. Still, cobalt systems can deactivate via particle growth, oxidation-reduction cycling, and carbon laydown when poorly dispersed or weakly anchored to the support [12]. Controlling metal dispersion, oxidation state, and metal-support interfacial chemistry is therefore central to realizing durable Co-based EDR catalysts [13].

Support selection provides a powerful level. Conventional oxides (Al_2O_3, SiO_2, ZrO_2, CeO_2, MgO) have each shown benefits on acid-base tuning, oxygen mobility, or thermal robustness [14], but sustainability and cost considerations motivate evaluation of alternative, waste-derived supports [15]. Palm-oil fuel ash (POFA) is generated in large quantities by the palm-oil milling industry, particularly in Southeast Asia. Typically landfilled, POFA is rich in amorphous silica and contains alkali and alkaline-earth species that may confer basicity and CO_2 activation sites when properly conditioned [16]. Acid washing and calcination can remove deleterious metals and organics while opening mesoporosity, yielding a low-cost, silica-rich scaffold with potential catalytic utility [17]. Valorizing POFA as a support both diverts an agricultural residue from disposal and reduces the embedded energy of catalyst manufacture, aligning with circular bioeconomy goals. Despite these advantages, systematic studies of cobalt deposition on POFA for high-temperature reforming remain scarce [18].

Preliminary work on biomass-ash supports suggests that metal loading exerts a non-linear influence on performance: loadings too low limit turnover due to insufficient active-site density, whereas excessive coverage promotes pore blockage, agglomeration, and transport limitations that accelerate deactivation [19]. Moreover, ash composition variability (Si, K, Ca, Fe, P) can mediate metal-support bonding and alter redox behaviour under reforming conditions [20]. A rigorous loading study, coupled with comprehensive physicochemical characterization, is needed to delineate the structure–function relationships governing activity, syngas selectivity, and stability in EDR [21-22].

Systematic studies of cobalt-loaded POFA for ethanol dry reforming are still lacking, though, especially when it comes to how cobalt loading affects syngas productivity, catalyst stability, and dispersion at high reforming temperatures [23]. The majority of earlier research has concentrated on Ni-based systems or traditional oxide supports, which has left a knowledge gap regarding the optimization of cobalt on waste-derived silica matrices and its function in preventing deactivation while preserving catalytic accessibility [24,25].

In order to maximize cobalt dispersion and determine the composition that offers the best balance between activity, hydrogen yield, and stability during ethanol dry reforming at 750 °C, this study prepares a series of cobalt-loaded POFA (Co/POFA) catalysts with different metal loadings (5–20 wt%). By establishing structure-function relationships between physicochemical properties and catalytic performance, this work supports the logical design of inexpensive reforming catalysts derived from waste for sustainable syngas production.

2. Materials and Methods

2.1 Materials

Palm-oil fuel ash (POFA) was selected as the silica-rich support for catalyst synthesis. Cobalt(II) nitrate hexahydrate ($Co(NO_3)_2 \cdot 6H_2O$, 98 %, Sigma-Aldrich, Malaysia) served as the metal precursor. The raw POFA was pre-treated with 30 wt% hydrochloric acid to leach residual metal ions, silica fines, and carbonaceous debris. The slurry was subsequently rinsed with deionized water until the pH reached neutral and dried at 105 °C overnight. Before catalytic testing, the impregnated samples were activated in situ by flowing hydrogen (99.9 %) at 500 °C for 2 h. High-purity nitrogen (99.9 %) was used to purge the fixed-bed reactor and establish an inert atmosphere, while carbon dioxide (99.5 %) was co-fed with ethanol (75 %, Sigma-Aldrich) during the ethanol dry-reforming experiments.

2.2 Preparation of Co/POFA Catalyst

Raw POFA was collected from the LCASB palm-oil mill (Lepar, Pahang, Malaysia). The ash (solid:liquid = 1:10) was leached in 30 wt% HCl under vigorous magnetic stirring for 3 h to remove residual metals and carbonaceous matter. It was then filtered through 150 mm qualitative paper and washed with deionized water at 80 °C until the pH reached neutrality. The solid was dried overnight at 105 °C and calcined at 600 °C for 6 h (Carbolite CWF-1200), then allowed to cool in situ. Cobalt was introduced by incipient-wetness impregnation: $Co(NO_3)_2 \cdot 6H_2O$ (98 %, Sigma-Aldrich) was dissolved in 50 mL deionized water to yield nominal cobalt loadings of 5, 10, 15, and 20 wt %. The precursor solution was added dropwise to 16 g of pre-treated POFA while stirring, followed by ultrasonication at 80 °C for 1 h to ensure homogeneous dispersion. The impregnated material was dried at 110 °C overnight, lightly ground, and calcined at 500 °C for 6 h. After cooling, the catalyst was pressed into pellets, crushed, and sieved to 1–2 mm particles, which were stored in airtight containers pending characterization and reaction testing.

2.3 Characterization of Catalyst

Catalyst characterisation was undertaken with a suite of complementary techniques. Fourier-transform infrared spectroscopy (FT-IR, Nicolet iS10, Thermo Scientific) was employed in the 4000-400 cm^{-1} region to identify surface functional [22] groups and probe metal-support interactions as a function of cobalt loading. Textural properties were obtained from N_2 adsorption-desorption isotherms at -196 °C using a Micromeritics ASAP 2020 Plus analyzer. Specific surface area was calculated by the Brunauer-Emmett-Teller (BET) method, while pore volume and diameter were derived from Barrett-Joyner-Halenda (BJH) analysis. Thermogravimetric analysis (TGA Q500, TA Instruments) of spent catalysts recovered after 5 h of ethanol dry reforming was carried out under air from 50 to 750 °C (10 °C.min^{-1}) to quantify mass losses associated with carbon deposition and assess structural stability.

2.4 Ethanol Dry Reforming Reaction

The fixed-bed quartz reactor was first assembled and leak-tested by purging with hydrogen (40 mL.min^{-1}) at 600 °C for 30 min. A 50 mL charge of ethanol was loaded into a glass syringe and fed with a precision syringe pump (KL-602, KellyMed) at 1.4 mL.h^{-1} to ensure complete vaporisation upstream of the catalyst bed (Figure 1). After the hydrogen purge, the feed was switched to a CO_2/N_2 mixture (10.7 mL.min^{-1} and 40 mL.min^{-1}, respectively) at 1 bar, and the furnace temperature was raised to 750 °C to initiate the ethanol dry-reforming reaction. Total volumetric flow was verified at the start and hourly intervals with a bubble flow meter, while effluent gases were collected every 60 min in 0.5 L Tedlar sampling bags (Restek) for an 8 min period. Each run was conducted for 5 h, and the protocol was repeated for all cobalt loadings. Product gases were quantified by gas chromatography [23] (GC 6890, Agilent) equipped with thermal conductivity detectors (TCD). A thermal conductivity detector (TCD)-equipped Agilent 6890 gas chromatograph was used to analyze the gaseous reaction products. Packed columns appropriate for permanent gases were used for gas separation (e.g., molecular sieve and Porapak Q columns). To ensure quantitative accuracy, certified standard gas mixtures were used for calibration before experiments began. H_2, CO, CO_2, and CH_4

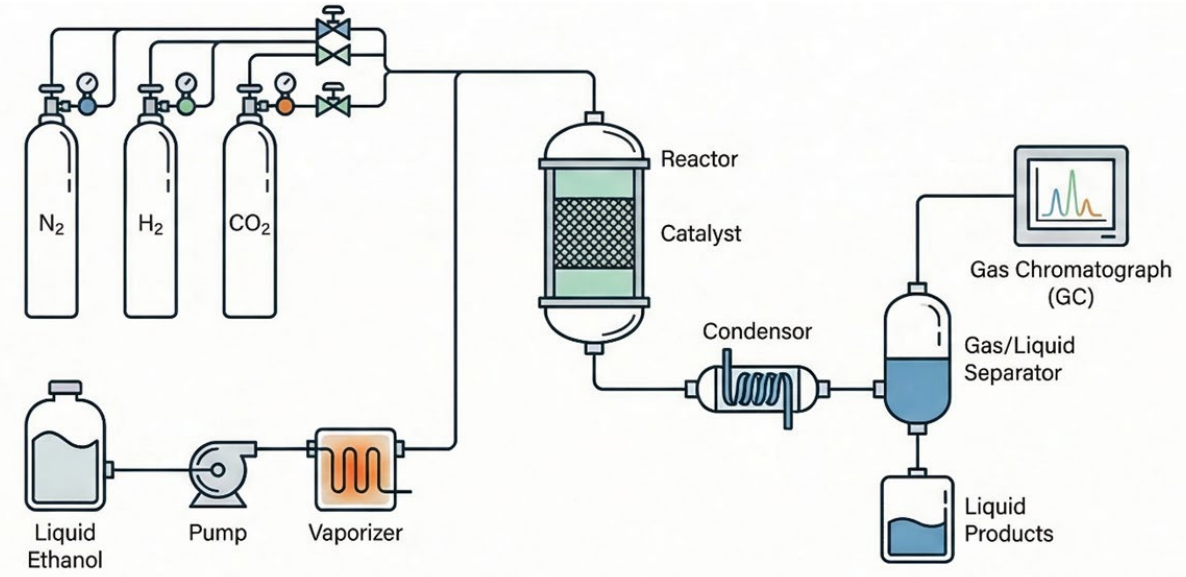

Figure 1. Schematic diagram of the EDR over Co/POFA catalyst.

concentrations were measured, and ethanol and CO_2 conversions, along with product yields, were computed using the molar flow rates at the inlet and outlet. Since the reactor used high-temperature vapor-phase reforming, the liquid products were insignificant and could not be measured.

3. Results and Discussion

3.1 Brunauer Emmett Teller (BET)

The progressive incorporation of cobalt onto the POFA support markedly altered its textural properties (Table 1). Surface area declined almost linearly from 15.18 $m^2.g^{-1}$ at 5 Co/POFA to 4.62 $m^2.g^{-1}$ at 20 Co/POFA, accompanied by concomitant reductions in pore volume from 0.0398 to 0.0252 $cm^3.g^{-1}$ and mean pore diameter from 11.67 to 9.46 nm. These trends signify partial pore filling and blockage by cobalt oxide clusters that nucleate preferentially within the larger mesopores of the ash-derived silica matrix. Similar losses in accessible surface following incipient-wetness impregnation [24] have been reported for bio-silica-based catalysts, where metal loadings beyond the percolation threshold occlude diffusion pathways and curtail nitrogen uptake at low relative pressures. Hence, while higher cobalt contents provide a greater density of potential active sites, they do so at the expense of overall porosity and external surface exposure.

Nitrogen-sorption isotherms for all samples exhibit type IV profiles with hysteresis at high relative pressure, confirming a mesoporous framework (Figure 2). The isotherm of the 5 Co/POFA material shows a shallow adsorption branch and the smallest capillary condensation step, consistent with its higher BET area yet limited mesopore volume. Increasing cobalt loading shifts the entire isotherm upward and intensifies the steep rise near $p/p^0 \approx 0.95$, indicative of cooperative filling of widened mesopores and emerging interparticle voids created by cobalt agglomerates. The 20 Co/POFA catalyst displays the highest adsorbed quantity above $p/p^0 \approx 0.8$ despite its low surface area, suggesting that large secondary pores and macropore throats dominate gas uptake in this regime, whereas micropore-level contributions-critical to BET calculations, are largely lost through pore blockage.

From a catalytic standpoint, an optimal balance is expected between metal dispersion and transport accessibility. The precipitous textural collapse at 20 Co/POFA is likely to limit active-site utilization and promote intra-particle diffusion resistances during ethanol dry reforming, while the relatively modest surface areas of the 5 Co/POFA and 10 Co/POFA samples may still sustain adequate dispersion without excessive pore occlusion. The 15 Co/POFA catalyst, exhibiting intermediate surface area (11.87 $m^2.g^{-1}$) and pore volume (0.0367 $cm^3.g^{-1}$) together with an enlarged mesopore network, should therefore provide the most favourable compromise to ensuring sufficient cobalt surface density for H-C-O bond activation while maintaining gaseous reactant and product flux, thus underpinning its anticipated superior syngas productivity in subsequent performance tests.

Table 1. BET analysis for physical properties of the catalyst.

Co loading (wt%)	BET surface area (m^2/g)	Pore volume (cm^3/g)	Mean pore diameter (nm)
5 Co/POFA	15.18	0.0398	11.67
10 Co/POFA	13.76	0.0357	10.83
15 Co/POFA	11.87	0.0367	10.23
20 Co/POFA	4.62	0.0252	9.46

3.2. Fourier Transform Infrared Spectroscopy (FTIR)

The low-frequency window of the FT-IR spectra (340-1940 cm^{-1}, Figure 3) is dominated by a band at ~840 cm^{-1} that is characteristic of the symmetric stretching of Si-O-Si rings in silica-rich ashes. Its persistence across all samples confirms retention of the POFA framework after impregnation, yet the gradual attenuation of band intensity and the slight red-shift from 836.9 cm^{-1} (10 Co/POFA) to 840.8 cm^{-1} (≥ 15 Co/POFA) signify progressive occupation of surface silanols by cobalt species. The concomitant suppression of the neighbouring overtone envelope (900-1100

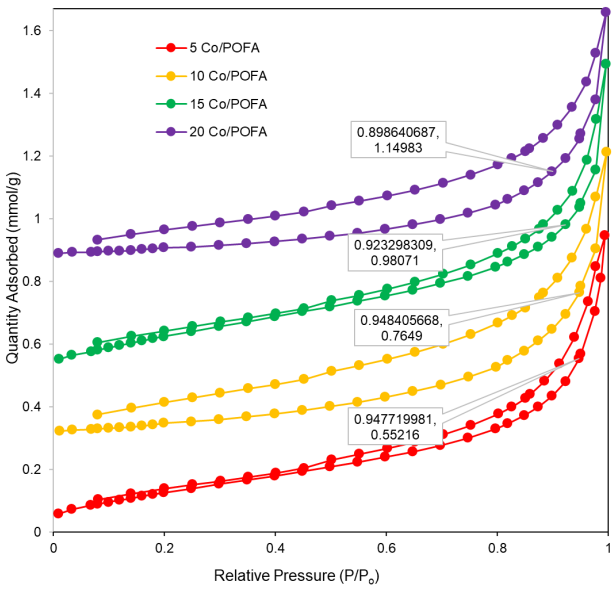

Figure 2. Isotherm tabular report for adsorption-desorption of catalyst 5 Co/POFA, 10 Co/POFA, 15 Co/POFA, 20 Co/POFA.

cm^{-1}, not shown) implies the formation of Co-O-Si linkages or nascent cobalt silicate domains, evidencing strong metal-support interactions that are beneficial for thermal stability under reforming conditions. The fact that no new absorptions attributable to residual nitrate (typically 1380 cm^{-1}) are observed confirms the efficacy of the calcination protocol in eliminating precursor anions, thereby avoiding parasitic oxygen release during reaction.

In the higher-frequency region (2000-3800 cm^{-1}, Figure 3) each catalyst displays a narrow absorption at ~215x cm^{-1} whose position shifts systematically from 2156 cm^{-1} (5 Co/POFA) to 2148 cm^{-1} (20 Co/POFA), tentatively assigned to linearly adsorbed CO on Co^{2+}/Co^{3+} sites generated during sample handling. The down-shift with loading reflects an increasing electron density on cobalt, consistent with the incipient formation of highly dispersed CoO_x clusters that are less electron-withdrawing than isolated ions. Meanwhile, the broad O-H stretching envelope centred at 3540-3522 cm^{-1} narrows and shifts to lower wavenumber as cobalt content rises, indicating consumption of surface silanols and the development of hydrogen-bonded water associated with cobalt oxide/hydroxide domains. Collectively, the spectroscopic evidence corroborates the textural data, revealing that cobalt loadings above 15 wt % generate extensive Co-O-Si connectivity while preserving a sufficient population of hydroxyl groups necessary for ethanol adsorption, an interplay expected to underpin the superior syngas productivity observed for the optimized 15 Co/POFA formulation.

Taken together, these findings demonstrate strong metal-support interactions that anchor cobalt species while preserving a hierarchically mesoporous network. Among the series, the 15 Co/POFA sample balances cobalt dispersion with accessible porosity, providing a favourable platform for syngas production via ethanol dry reforming.

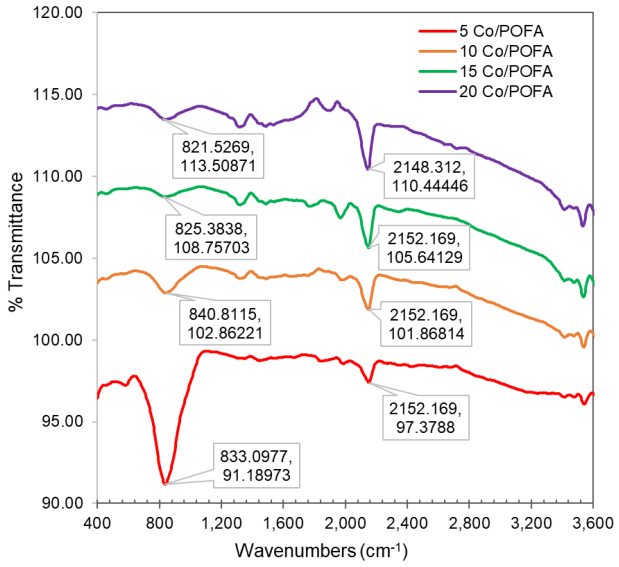

Figure 3. FT-IR spectrum adsorbent from various catalyst loading 340 cm^{-1} – 3800 cm^{-1} wavelength.

The current study focuses on connecting catalytic behavior with readily accessible physicochemical properties derived from nitrogen physisorption, FT-IR, and post-reaction TGA, even though sophisticated techniques like XRD or XPS could offer more insight into cobalt crystallinity and oxidation states. The observed activity trends are in line with reports in the literature that indicate the main factors influencing reforming stability are cobalt dispersion, pore accessibility, and resistance to carbon accumulation. Previous research has shown that while intermediate loading increases metal accessibility and durability, excessive metal loading encourages particle agglomeration and diffusion limitations. Therefore, the combined catalytic and characterization results obtained here are adequate to explain the structure–performance relationships governing Co/POFA catalysts in ethanol dry reforming, even though additional structural analysis could improve mechanistic interpretation.

3.3. Catalytic Activity on Ethanol Dry Reforming

Time-on-stream data (Figure 4) show that EDR performance is strongly dependent on cobalt loading. The 15 Co/POFA catalyst delivered the highest initial ethanol and CO_2 conversions (≈72 % and 80 %, respectively) and maintained the greatest fraction of its activity after 5 h on stream (≈50 % ethanol; 68 % CO_2), whereas the 20 Co/POFA material, despite its higher nominal metal content, decayed most rapidly and stabilised at substantially lower conversions (~30 % ethanol; ~52 % CO_2). The 10 Co/POFA and 5 Co/POFA samples reached intermediate (~45 %) and lower (~35 %) ethanol conversions, respectively, with correspondingly lower CO_2 utilisation. These trends indicate that an intermediate cobalt inventory maximises the number of accessible redox/metallic sites without incurring severe transport or thermal penalties.

Hydrogen productivity followed a similar hierarchy. The 15 Co/POFA catalyst started near 60 % H_2 yield and declined gently to ~48 % at 5 h, preserving the highest steady-state level among the series. In contrast, the 20 Co/POFA sample exhibited a sharp early drop from ~50 % to ~32 % within the first hour before levelling, whereas the 10 C/POFA and 5 Co/POFA catalysts converged near ~45 % and ~40 %, respectively. The abrupt loss for 20 Co/POFA suggests rapid masking of cobalt sites, likely via coke emergence within constricted pores or agglomeration of large Co

domains. While the sustained H_2 evolution over 15 Co/POFA indicates superior resistance to such blockage.

Selectivity behaviour provides additional insight. CO yields diverged from H_2: after an initial transient, the low-loading 5 Co/POFA catalyst produced the highest and most persistent CO fraction (~42 %), whereas the 15 Co/POFA and 20 Co/POFA samples trended lower (30–40 %). Lower cobalt density evidently suppresses secondary hydrogenation and shift pathways that would otherwise consume CO, while larger cobalt ensembles on the higher-loading samples can promote CO hydrogenation to CH_4 and re-oxidative routes that dilute CO selectivity. Thus, overall reforming activity (best at 15 Co/POFA catalyst) and CO selectivity (favoured at 5 Co/POFA catalyst) do not peak at the same metal loading, underscoring the tunability of syngas composition through cobalt dispersion.

Correlating these kinetic outcomes with physicochemical characterisation clarifies the origin of the loading optimum. Nitrogen sorption revealed progressive loss of surface area and pore volume with increasing cobalt content; nevertheless, the 15 Co/POFA material retained sufficient mesoporosity (BET ~11.9 $m^2.g^{-1}$; mean pore ~103 Å) to accommodate well-dispersed CoO_x clusters while preserving gas transport. FT-IR evidence of Co-O-Si interfacial bonding at this loading suggests strong metal anchoring that mitigates sintering and provides labile oxygen capable of oxidising emergent carbon species under CO_2-rich feeds. By comparison, the 5 Co/POFA catalyst, though texturally open, contains too few cobalt sites for sustained turnover, whereas the 20 Co/POFA sample displays symptoms of pore blockage and cobalt agglomeration that restrict access and hasten deactivation.

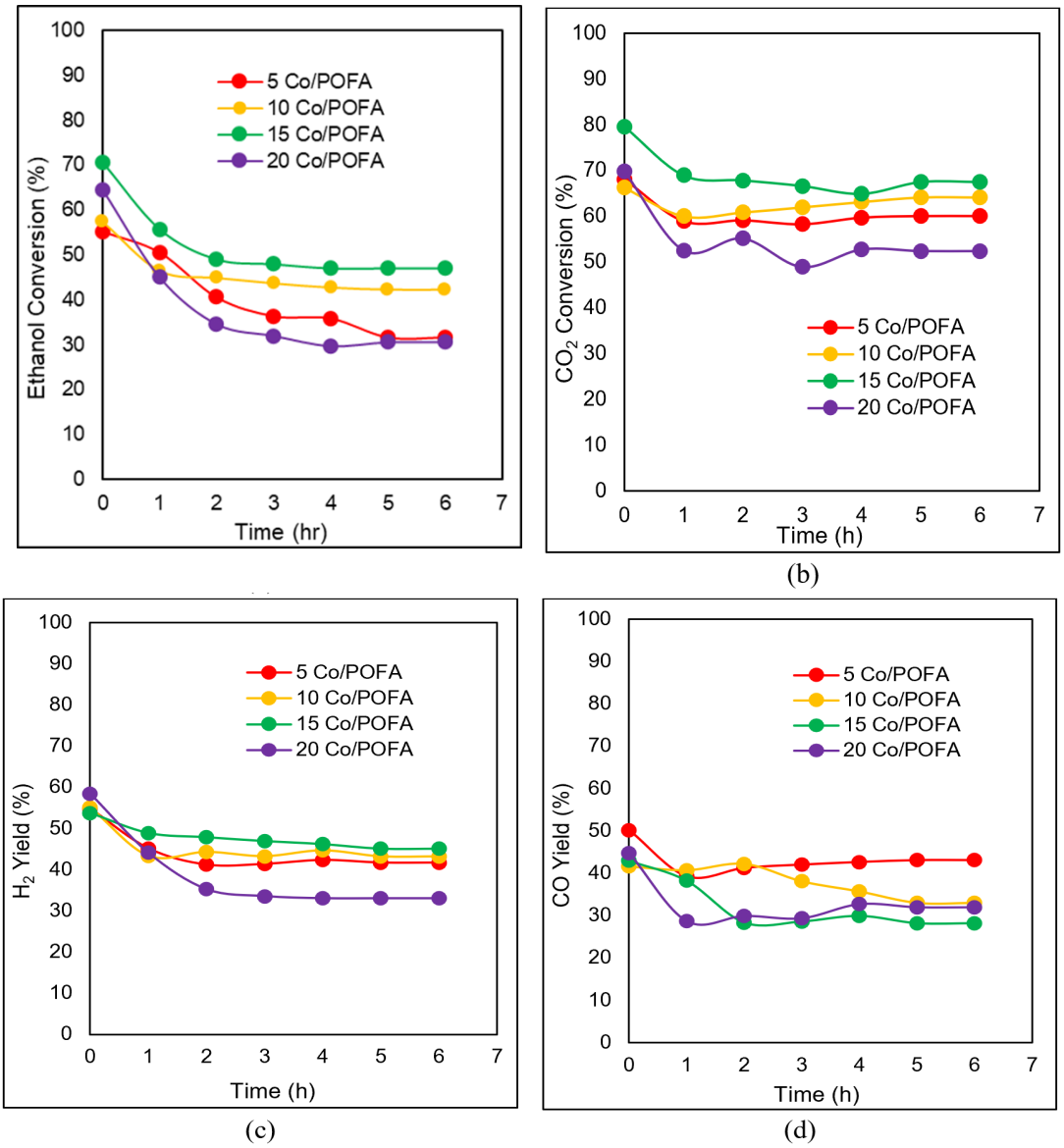

Figure 4. (a) Ethanol conversion, (b) CO_2 conversion, (c) H_2 yield, (d) CO yield on different Co loadings.

Differences in stability are consistent with these structure–function relationships. The steep early decline in ethanol conversion for 20 Co/POFA points to diffusion-limited carbon laydown within blocked pores, while the more gradual decay observed for the 15 Co/POFA catalyst suggests that its interconnected mesopores and anchored cobalt domains facilitate removal or gasification of heavy intermediates before they evolve into deactivating coke. The 5 Co/POFA and 10 Co/POFA materials deactivate more slowly but cumulatively, behaviour that may arise from progressive growth or oxidation–reduction cycling of smaller, less well-anchored cobalt particles.

Integrating activity, selectivity, textural, spectroscopic, and thermal evidence demonstrates that a cobalt loading near 15 wt % on acid-treated, calcined POFA yields the most robust balance of active-site density, metal-support intimacy, and mesopore accessibility required for high and durable syngas productivity under EDR. Sub-optimal (5 Co/POFA) loading is intrinsically site-limited and prone to CO-rich but H_2-lean product streams, whereas excessive loading (20 Co/POFA) invites pore occlusion, cobalt agglomeration, and rapid deactivation that erode both conversion and H_2 yield despite low measured coke accumulation. Tailoring cobalt dispersion within the POFA mesostructure is therefore pivotal to engineering low-cost, waste-derived reforming catalysts capable of sustained CO_2 valorisation and renewable syngas generation.

When compared to previously published catalysts for ethanol dry reforming, the optimized 15 wt% Co/POFA catalyst performs superbly. Ni-based systems that are supported by conventional oxides usually convert 60–75% of ethanol at comparable temperatures, but they frequently experience rapid deactivation and significant coke deposition. Although many of the conversions reported in recent studies on mixed oxide catalysts require more complicated synthesis routes or higher metal loadings to maintain stability, similar conversions have been reported. Similar conversion levels are achieved by the Co/POFA catalyst created in this work, which also benefits from a waste-derived support that encourages dispersion and lowers carbon formation. The potential of conditioned POFA as a low-cost, efficient support that can maintain syngas production under challenging reforming conditions and stabilize cobalt active sites is demonstrated by these results.

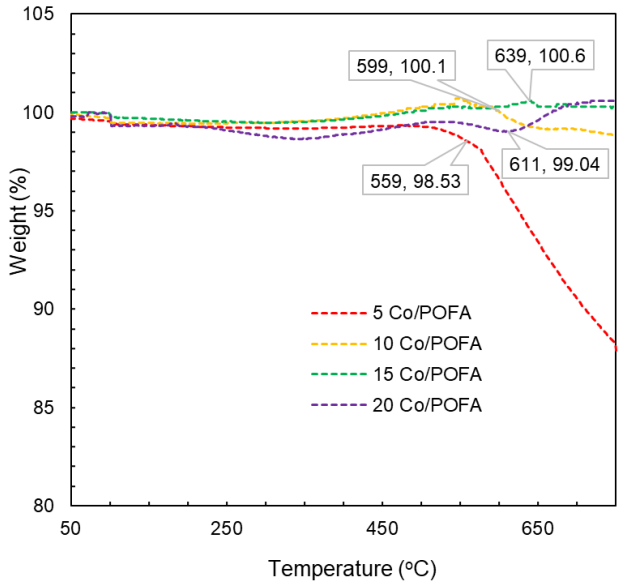

Figure 5. Analysis weight loss of the spent catalyst using thermal gravimetric analysis.

3.4 Thermal Gravimetric Analysis (TGA)

Thermogravimetric traces of the spent Co/POFA catalysts (Figure 5) furnish additional insight into the deactivation pathways inferred from the activity tests. All samples exhibit a minor mass loss (< 1 %) below 200 °C, attributable to desorption of physisorbed water and low-boiling oxygenates. Beyond this region, the behaviour diverges sharply with cobalt loading. The 5 Co/POFA catalyst undergoes a pronounced, continuous loss commencing at ≈ 500 °C and culminating in an overall 11 % decrease at 750 °C, a temperature range typical for the combustion of graphitic carbon. The magnitude of the loss confirms that extensive coke was laid down during reaction, consistent with the rapid decline in ethanol conversion and the concomitant elevation in CO selectivity observed for this sample. Limited cobalt surface density and weaker metal–support anchoring, as evidenced by its highest BET area and the faintest Co-O-Si IR signature, favour filamentous carbon growth and hinder its in-situ gasification.

By contrast, the 10 Co/POFA, 15 Co/POFA and 20 Co/POFA formulations display net mass changes of –1 %, ~0 % and +1–2 %, respectively. The slight weight gain for the two higher loadings is ascribed to oxidation of residual metallic Co to Co_3O_4, which offsets or exceeds the modest coke burn-off. The near-zero change for 15 Co/POFA confirms that carbon deposition was effectively suppressed while cobalt oxidation remained limited an outcome that mirrors its superior catalytic stability. The 20 Co/POFA catalyst, though essentially coke-free, nonetheless lost activity during EDR; this finding implicates sintering and pore blockage, not coking, as the dominant deactivation route when cobalt coverage surpasses the optimal threshold and agglomeration is promoted [25].

TGA corroborates the structure performance relationships derived from BET, FT-IR and kinetic data. Excessively low cobalt loading (5 Co/POFA) leads to significant coke accumulation

and attendant activity loss, whereas excessive loading (20 Co/POFA) suppresses coke but invites particle sintering, undermining turnover despite minimal weight loss. An intermediate cobalt content of 15 Co/POFA minimises both carbon deposition and cobalt oxidation, preserving active-site accessibility and sustaining high ethanol and CO_2 conversions. Thus, thermal-stability profiling reinforces that the synergy between balanced metal dispersion, mesoporous architecture and robust Co-O-Si bonding is pivotal for long-lived syngas production over Co/POFA catalysts in ethanol dry reforming. Following the reaction, the samples were recovered, dried, and subjected to direct TGA analysis without any additional processing.

4. Conclusion

Palm-oil fuel ash (POFA), after acid washing and calcination, functions as an effective low-cost, waste-derived support for cobalt in ethanol dry reforming (EDR). Systematic variation of cobalt loading (5-20 wt%) showed a pronounced structure-performance optimum: although increasing Co progressively reduced surface area and pore volume, a 15 Co/POFA coating preserved sufficient mesoporosity and formed strong Co-O-Si interfacial linkages that stabilized the active phase. Under EDR at 750 °C, 15 Co/POFA delivered the highest and most durable performance (initial ~72 % ethanol and ~80 % CO_2 conversion; ~50 % and ~68 % after 5 h) and sustained the greatest H_2 yield (~48 %). Lower loading (5 Co/POFA) was site-limited and accumulated substantial coke, while excessive loading (20 Co/POFA) suffered rapid deactivation attributed to pore blockage and cobalt agglomeration despite minimal carbon deposition. These results demonstrate that tuning cobalt dispersion within the POFA mesostructure is critical to balancing activity, selectivity, and stability. Optimized Co/POFA catalysts therefore provide a practical route to valorize agricultural residues, co-utilize bioethanol and CO_2, and generate flexible syngas streams for downstream low-carbon fuels synthesis.

Acknowledgment

This study was supported by grant UIC241526/RDU242725, the International Matching Grant from Universitas Ahmad Dahlan, and Universiti Malaysia Pahang Al-Sultan Abdullah. The authors sincerely appreciate the research facilities and technical support provided by Universiti Malaysia Pahang Al-Sultan Abdullah.

CRedit Author Statement

Author Contributions: Mohamad Irfan Nordin: Conceptualization, Methodology, Investigation, Formal Analysis, Data Curation, Writing, Writing-Original Draft Preparation; Nurul Ainirazali: Validation, Supervision, Project Administration, Writing, Review and Editing; Asmida Ideris: Conceptualization, Methodology, Discussion, Writing, Review and Editing; Muhammad Shahim Azim Razat: Investigation, Data Curation, Formal Analysis, Contributing Ideas and Discussion; Siti Jamilatun: Funding Acquisition, Resources, Discussion, Contributing Ideas; Joko Pitoyo: Funding Acquisition, Resources, Discussion, Contributing Ideas; Utaminingsih Linarti: Funding Acquisition, Resources, Discussion, Contributing Ideas. All authors have read and agreed to the published version of the manuscript.

References

[1] Abdulrasheed, A., Jalil, A.A., Gambo, Y., Ibrahim, M., Hambali, H.U., Hamid, M.Y.S. (2019). A review on catalyst development for dry reforming of methane to syngas: recent advances. *Renew. Sustain. Energy Rev.*, 108, 175–193. DOI: 10.1016/j.rser.2019.03.054.

[2] Wijayasekera, S.C., Hewage, K., Siddiqui, O., Hettiaratchi, P., Sadiq, R. (2022) Waste-to-hydrogen technologies: Techno-economic and socio-environmental sustainability. *Int J Hydrogen Energy*. 47, 5842–5870. DOI: 10.1016/j.ijhydene.2021.11.226

[3] Zhang, K. (2024). The role of hydrogen in the energy transition of the oil and gas industry. *Energy Rev.*, 100090. DOI: 10.1016/j.enrev.2024.100090.

[4] Li, T., Li, F., Nginyo, J., Cai, W., Yu, B. (2023). Syngas production through dry reforming of ethanol over Co@SiO2 catalysts: effect of SiO2 shell thickness. *Mol. Catal.*, 547, 113307. DOI: 10.1016/j.mcat.2023.113307.

[5] Bahari, A., Ainirazali, N. (2016). Hydrogen-rich syngas production from ethanol dry reforming on La-doped Ni/Al2O3 catalysts: effect of promoter loading. *Procedia Eng.*, 148, 654–661. DOI: 10.1016/j.proeng.2016.06.531.

[6] Khlusova, K. (2024). High-performance Ni/Al2O3-(Zr+Ce)O2 catalysts for syngas production via ethanol dry reforming. *Fuel*, 376, 132685. DOI: 10.1016/j.fuel.2024.132685.

[7] Shafiqah, M.N., Siang, T.J., Kumar, P.S., et al. (2022). Advanced catalysts and effect of operating parameters in ethanol dry reforming for hydrogen generation: a review. *Environ. Chem. Lett.*, 20(3), 1695–1718. DOI: 10.1007/s10311-022-01394-0.

[8] Montero, C., Ochoa, A., Castaño, P., Bilbao, J., Gayubo, A.G. (2015). Monitoring Ni⁰ and coke evolution during the deactivation of a Ni/La_2O_3–αAl_2O_3 catalyst in ethanol steam reforming in a fluidized bed. *J. Catal.*, 331, 181–192. DOI: 10.1016/j.jcat.2015.08.005.

[9] Tian, X. (2022). Effect of air introduction on filamentous coke during CO2 reforming of tar with core-shell catalysts. *J. Anal. Appl. Pyrolysis*, 168, 105765. DOI: 10.1016/j.jaap.2022.105765.

[10] Jaramillo-Baquero, M., Dieuzeide, M.L., Múnera, J., Cornaglia, L. (2025). Highly dispersed and stable Ni catalysts for hydrogen production via steam reforming of ethanol. *Chem. Eng. J.*, 523, 168482. DOI: 10.1016/j.cej.2025.168482.

[11] Aramouni, N.A.K., Zeaiter, J., Kwapinski, W., Leahy, J.J., Ahmad, M.N. (2021). Trimetallic Ni-Co-Ru catalyst for the dry reforming of methane: effect of the Ni/Co ratio and calcination temperature. *Fuel*, 300, 120950. DOI: 10.1016/j.fuel.2021.120950.

[12] Zhao, Y., Geng, J., Cai, Y., Wang, C., Zhang, Q., Wang, H. (2019). One-step synthesis of metallic Ni–C/Al2O3 directly applied for CO2 reforming of CH4. *Int. J. Hydrogen Energy*, 44(39), 21651–21658. DOI: 10.1016/j.ijhydene.2019.06.113.

[13] Fayaz, F., He, C., Goel, A., Rintala, J., Konttinen, J. (2024). Oxidative ethanol dry reforming for syngas production over Co/Al2O3 catalysts: effect of reaction temperature. *Mater. Today Commun.*, 38, 107912. DOI: 10.1016/j.mtcomm.2023.105671.

[14] Chong, C.C. (2019). Hydrogen production via CO2 reforming of CH4 over low-cost Ni/SBA-15 from silica-rich palm oil fuel ash (POFA) waste. *Int. J. Hydrogen Energy*, 44(37), 20815–20825. DOI: 10.1016/j.ijhydene.2018.06.169.

[15] Eremeev, N., Hanna, S.A., Sadykov, V.A., Bespalko, Y.N. (2025). Ethanol dry reforming into synthesis gas: effect of oxygen mobility and reactivity. *Sustain. Energy Fuels*, 9, 4554–4587. DOI: 10.1039/D5SE00359H.

[16] Hubadillah, S.K. (2019). Influence of pre-treatment temperature of palm oil fuel ash on properties and performance of green ceramic hollow fiber membranes. *Sep. Purif. Technol.*, 222, 264–277. DOI: 10.1016/j.seppur.2019.04.046.

[17] Esquinas, A., Ledesma, E., Otero, R., Jiménez, J., Fernández, J. (2018). Mechanical behaviour of self-compacting concrete made with non-conforming fly ash from coal-fired power plants. *Constr. Build. Mater.*, 182, 385–398. DOI: 10.1016/j.conbuildmat.2018.06.094.

[18] Montero, C., Ochoa, A., Castaño, P., Bilbao, J., Gayubo, A.G. (2015). Monitoring Ni⁰ and coke evolution during deactivation of a Ni/La2O3–αAl2O3 catalyst in ethanol steam reforming. *J. Catal.*, 331, 181–192. DOI: 10.1016/j.jcat.2015.08.005.

[19] Wang, X. (2021). Ultrasonic-assisted hydrothermal synthesis of cobalt oxide/nitrogen-doped graphene oxide hybrid as oxygen reduction reaction catalyst. *Ultrason. Sonochem.*, 72, 105457. DOI: 10.1016/j.ultsonch.2020.105457.

[20] Sun, Y. (2023). Experimental parameters for preparation of Mn/TiO2 catalysts by ultrasonic spray pyrolysis method. *Chem. Phys. Impact*, 7, 100258. DOI: 10.1016/j.chphi.2023.100258.

[21] Xin, S. (2021). High efficiency heterogeneous Fenton-like catalyst biochar modified CuFeO2 for degradation of tetracycline. *Appl. Catal. B Environ.*, 280, 119386. DOI: 10.1016/j.apcatb.2020.119386.

[22] Ainirazali, N. (2019). Influence of impregnation assisted methods of Ni/SBA-15 for production of hydrogen via dry reforming of methane. *Int. J. Hydrogen Energy*, 45(36), 18426–18439. DOI: 10.1016/j.ijhydene.2019.09.089.

[23] Shah, M.N., Patel, N.H., Shah, D.D., Mehta, P. (2021). FTIR: important tool to investigate chemical bond formation in polycrystalline xBaTiO3–(1-x)BiFeO3. *Mater. Today Proc.*, 47, 616–620. DOI: 10.1016/j.matpr.2020.11.402.

[24] Williams, P. (2020). Comparison of offline SPE–GC–MS and online HS–SPME–GC–MS method for analysis of volatile terpenoids in wine. *Molecules*, 25(3), 657. DOI: 10.3390/molecules25030657.

[25] Mambetova, M., Anissova, M., Myltykbayeva, L., Makayeva, N., Dossumov, K., Yergaziyeva, G. (2025). Catalyst development for dry reforming of methane and ethanol into syngas: recent advances and perspectives. *Appl. Sci.*, 15(19), 10722. DOI: 10.3390/app151910722..